Naderi, M.; Bahramara, S.; Khayat, Y.; Bevrani, Hassan

Article

Optimal planning in a developing industrial microgrid with sensitive loads

Energy Reports

Provided in Cooperation with:
Elsevier

Suggested Citation: Naderi, M.; Bahramara, S.; Khayat, Y.; Bevrani, Hassan (2017) : Optimal planning in a developing industrial microgrid with sensitive loads, Energy Reports, ISSN 2352-4847, Elsevier, Amsterdam, Vol. 3, pp. 124-134, https://doi.org/10.1016/j.egyr.2017.08.004

Energy Reports 3 (2017) 124–134

Contents lists available at ScienceDirect

Energy Reports

journal homepage: www.elsevier.com/locate/egyr

Optimal planning in a developing industrial microgrid with sensitive loads

M. Naderi [a,*], S. Bahramara [b], Y. Khayat [a], H. Bevrani [a]

[a] Smart/Micro Grids Research Center, Department of Electrical and Computer Eng., University of Kurdistan, PO Box 416, Sanandaj, Iran
[b] Department of Electrical Engineering, Sanandaj Branch, Islamic Azad University, Sanandaj, Iran

HIGHLIGHTS

- Optimal microgrid planning for industrial estate as a new work.
- Enhancing power quality, reliability and security of CNC workshops (sensitive loads).
- Load forecasting in details considering the end users devices and load factors.
- Sensitivity analysis on uncertain parameters in details.

ARTICLE INFO

Article history:
Received 29 December 2016
Accepted 21 August 2017
Available online 12 September 2017

Keywords:
MG planning
CNC machine
RES penetration
HOMER
Reliability

ABSTRACT

Computer numerical control (CNC) machines are known as sensitive loads in industrial estates. These machines require reliable and qualified electricity in their often long work periods. Supplying these loads with distributed energy resources (DERs) in a microgrid (MG) can be done as an appropriate solution. The aim of this paper is to analyze the implementation potential of a real and developing MG in Shad-Abad industrial estate, Tehran, Iran. Three MG planning objectives are considered including assurance of sustainable and secure operation of CNC machines as sensitive loads, minimizing the costs of MG construction and operation, and using available capacities to penetrate the highest possible renewable energy sources (RESs) which subsequently results in decreasing the air pollutants specially carbon dioxide (CO_2). The HOMER (hybrid optimization model for electric renewable) software is used to specify the technical feasibility of MG planning and to select the best plan economically and environmentally. Different scenarios are considered in this regard to determine suitable capacity of production participants, and to assess the MG indices such as the reliability.

1. Introduction

Nowadays, one of the most important environmental issues is global warming and constantly-increased air pollution by fossil fuels (Leung et al., 2014). Over the past century, atmospheric CO_2 level has increased more than 39% in May 2013 with a corresponding increase in global surface temperature of about 0.8 °C (NOAA, 2016). RESs can be an appropriate solution for this problem according to the researchers and policy makers' outcomes (Ngan and Tan, 2012). Wind turbines (WTs), photovoltaic (PV) panels, geothermal power plants and other technologies are the best way to generate electrical energy without any air pollutions (Prodromidis and Coutelieris, 2010).

On the other hand, sensitive loads are increased due to industrialization, social welfare improvement and energy technologies development. The CNC machines have been known as very common and also sensitive loads in the lathing and milling industries in which computers play an integral role. These machines do lathe and mill operations with the precision of micrometer during uninterrupted hours. Variable frequency drives (VFDs) are applied to the CNC equipment to regulate the servo motors, control the axes motion, etc. All of these processes are required to highly-detailed components are created from raw materials. Due to the presence of VFDs as sensitive and expensive interfaces, continuous CNC work condition, and the importance of the produced components, CNC machines are considered as sensitive loads from the power supply point of view. Any issue corresponding to power quality concepts such as voltage sag, fluctuation, overvoltage and interruption can cause irreparable events such as accident of CNC machine's axes, the sensitive component failing or destroying, and the VFD burning. Each one of these events will be followed with financial damages, imposed on CNC workshop owners, while electrical distribution companies are responsible for supplying the

* Corresponding author.
E-mail address: m.naderi@eng.uok.ac.ir (M. Naderi).

http://dx.doi.org/10.1016/j.egyr.2017.08.004

Table 1
A typical CNC machine consumption in a normal working hour.

Electrical load type	Nominal capacity (kW)	Load factor (%)
X-axis servo motor	2	50
Y-axis servo motor	2	50
Z-axis servo motor	2	50
Spindle servo motor	11	100
Hydraulic pump motor	3	100
Lubrication pump motor	0.2	16
Cooling fan motor	0.5	100
Chip conveyor motor	1	20
Flood coolant motor	1	30
Total losses (drives, contactors etc.)	1	100

electricity with appropriate power quality. Refs. (Morinec, 2000, 2002; Vasconcellos et al., 2010) represent some ways to improve power quality in the presence of CNC machines as sensitive loads such as grounding. Nevertheless, providing an independent, secure and reliable supply may be better solution and should be studied.

DERs including conventional distributed generations, RESs, and energy storage sources are introduced as appropriate resources to meet the loads locally. These resources are integrated with local loads as MGs (Sorensen, 2011; Twidell and Weir, 2015; Botelho et al., 2016) which can operate in both grid-connected and islanded modes (Babazadeh and Karimi, 2013). As a solution, MGs undertake to facilitate the wide penetration and integration of RESs and energy storage devices into the power system in developing countries, increase feasibility of off-grid electrification, reduce system losses and greenhouse gas emissions, and increase the reliability (Louie, 2016; Manas, 2015; Li et al., 2016; Peerapong and Limmeechokchai, 2017; Kobayakawa and Kandpal, 2016). Due to their potential benefits of providing source, efficient, reliable, sustainable, and environmentally-friendly electricity from RESs, MGs are taken into account more than ever (Bevrani et al., 2017). MGs construction is growing in different areas like military regions, universities, industrial estates and etc. due to the mentioned reasons. The industrial estates are interested in because of their enormous greenhouse gasses emission and existence of sensitive loads such as induction furnaces and CNC machines. In fact, the importance of the sensitive loads is another reason to plan and construct an MG in the industrial estates.

One of the important issues in MG planning is determining the optimal size of its resources to meet the load so that the objective function is minimized/maximized and technical constraints are met. Economic, environmental, and reliability-based indices are used as objective functions in the planning formulation of the MGs. Different software and optimization techniques are used to optimal sizing of MGs in the literature. HOMER is the powerful software which is used by many researchers for optimal planning of MGs (Bahramara et al., 2016; Olatomiwa, 2016).

The main contributions of the presented work are summarized as follows:

- Optimal MG planning in the industrial estate is done which does not take account enough in the literature. The main idea is enhancing power quality, reliability and security of CNC workshops as sensitive loads by implementation of an MG.
- Load forecasting is done in details considering the end users devices and their load factors, while in the most previous studies, monthly average load consumption is only considered for simulation.
- Sensitivity analysis on uncertain parameters is done in details which this subject is not investigated well in the literature yet.

The rest of this paper is organized as follows. Section 2 presents the description of HOMER input parameters. In Section 3, system description and specification is presented. The economic analysis is prepared in Section 4. In Section 5, simulations are conducted and discussed. Finally, conclusion is done in Section 6.

Table 2
Consumption of a typical manual lathing/milling machine in a normal working hour.

Electrical load type	Nominal capacity (kW)	Load factor (%)
Common X and Z axes motor	5	100
Spindle motor	1	100
Flood coolant motor	0.5	30

2. Description of input parameters

The HOMER software needs some input parameters for simulation including load profile, solar radiation, wind resource, RESs capacity, initial costs per unit for each component, etc. These parameters is further enlarged in the following subsections.

2.1. Load profile of the CNC workshops set

In this study, a set of eight CNC workshops is selected as the total load to test the feasibility of the designed MG. This set is located in 11 Fath, Shad-Abad industrial estate, Tehran, Iran. Every workshop has certain and individual CNC machines and other equipment. However, all of them are similar in viewpoint of consumed energy type. Nevertheless, their energy consumptions are different. An average load is considered for all workshops instead of their different consumptions to facilitate the load estimation. In this study, based on the nearby workshops visit, the certain equipment and consumptions are considered for all workshops containing CNC machines, manual lathing/milling machines, lighting, and miscellaneous consumptions such as air-conditioning, computers, refrigerators, etc. On average, every workshop has three CNC machines, two manual lathe/milling machines, ten 46 W duplex lamps and 2 kW equivalent consumption of miscellaneous equipment. Since the majority of CNC machines whether milling or lathing are three-axis or can expand to it, they are considered three-axis on average in this paper. A typical consumption of a three-axis CNC is described in Table 1. In addition to the nominal capacity of a motor, its load factor is considered to show the real average time of motor involvement. Similarly, Table 2 shows the consumption of a typical manual lathing/milling machine. According to this detailed consumptions, the total consumption of a CNC workshop is calculated in Table 3. Finally, the maximum consumption of the eight workshops that is the peak load of the MG, is obtained 577.76 kW.

The CNC workshops as the MG loads work about simultaneously from 8 a.m. to 5 p.m. Therefore, consumption timing of CNC workshops with respect to each other is similar. On the other hand, the timing of different consumptions of each CNC workshop itself is similar on average. In addition, basic changes in the CNC workshops activities happen monthly and seasonally. All of these

Table 3
CNC workshop consumption in a normal working hour.

Electrical load type	Consumption calculation	Number	load (kW)
CNC machine	$(2+2+2)\times 0.5+(11+3+0.5+1)\times 1$ $+0.2\times 0.16+1\times 0.2+1\times 0.3=19$ kW	3	57
Manual lathing/milling machine	$(5+1)\times 1+0.5\times 0.3=6.15$ kW	2	12.30
Lighting	$2\times 0.046=0.092$ kW	10	0.92
Miscellaneous equipment	2 kW	–	2
Total CNC workshop load			72.22

Table 4
Daily load forecast data of the workshops set in July.

Time zone (h)	0–8	8–12	12–13	13–17	17–21	21–24
Percent of daily high load (Weekends) (%)	10 (3)	90 (27)	60 (18)	100 (30)	50 (15)	20 (6)
Weekday load (kW)	42.6	383.2	255.5	425.8	213	85.2
Weekend load (kW)	12.7	115	76.6	127.7	64	25.6

reasonable assumptions for the CNC workshops as the MG loads are applied in the form of daily and monthly consumption patterns in HOMER. However, overtimes and CNC continuous working in the range of one or two weeks or even one month, according to the performed project type, should be considered. This partial changes of the workshop activities is considered monthly too. Hence, one day per each month is selected as an agent of that month. Since CNC workshops have their minimum activity in weekends, their consumptions are considered thirty percent of weekdays. Finally, the data of 24 days (12 days for weekdays and 12 days for weekends) is imported to the HOMER as the annual data. Table 4 shows the typical data of daily load forecasting of the workshops set in July. Moreover, a sample of the daily load profile for both weekdays and weekends is shown in Fig. 1. It is noteworthy that the active working hours have shifted to the last hours of the evening, according to the real data. It has a negative effect on the optimal consumption, and also social welfare.

A random variability is given by the HOMER software to estimate the maximum and minimum variations of the input daily load profile from a certain day to other days and from a certain time-step to other time-steps. In this study, random changes, which are shown by day-to-day and time-step to time-step variability in the software, are set as 8% and 10% respectively. In fact, these numbers specify the variance of the consumption load as a random variable around its average amount determined by the input load profile. The scaled annual average energy demand of the CNC workshops set as simulated by HOMER software is 3294 kWh/day which is equivalent to 1.2 GWh/year.

2.2. Solar radiation and ambient temperature

The data of solar radiation and ambient temperature is achieved from National Aeronautics and Space Administrative (NASA) (Surface meteorology, 2016). It is 22-year monthly average data. Fig. 2(a) shows the solar radiation data inputs, used in the HOMER software, as well as the clearness index of the solar radiation. The clearness index is automatically calculated by HOMER when the monthly radiation data is entered (Lau et al., 2010). The latitude and longitude of Shad-Abad are 33°63′N and 46°41′E, respectively. The solar irradiance changes from 3.03 kWh/m^2/day to 5.96 kWh/m^2/day. The annual average of the solar radiation is estimated as 6.07 kWh/m^2/day according to the clearness index. As it can be seen from Fig. 2(a), solar radiation is high and sufficient from May to September, while it is low relatively (between 3 and 4 kWh/m^2/day) for other months. The data of the ambient temperature is shown in Fig. 2(b). It is the monthly average air temperature at 10m above the surface of the earth for the location of Shad-Abad, Iran. The HOMER uses the data of solar radiation and ambient temperature to calculate the output power of PV panels in each time step.

2.3. Wind speed

The wind speed data is obtained from NASA database for the location of Shad-Abad, Iran (Surface meteorology, 2016). It is 22-year monthly average wind speed data which is measured at 10m above the surface of earth. The wind speed changes from 3.4 m/s to 4.5 m/s. The highest wind speed occurs in May–September, although the monthly wind speed changes are not sensible in comparison of the solar radiation. The parameters Weibull k, auto-correlation factor, diurnal pattern strength, and hour of peak wind speed have been employed by the HOMER to describe the randomness of the wind speed. The parameter Weibull k, is a measure of the long term distribution of the wind speed over a year, whereas the auto-correlation factor represents the hour-to-hour randomness of the wind speed. The diurnal pattern strength is a measure of how strongly the wind speed depends on the time of day, and finally the hour of peak wind speed is the time of day that tends to be windiest on average (HOMER help, 2016). A high diurnal pattern strength value shows that there is a relatively strong dependence on the time of day and vice versa (Demiroren and Yilmaz, 2010). In this study, the parameters Weibull (k), auto-correlation factor and diurnal pattern strength are considered to be 2.5, 0.85 and 0.25, respectively, and the hour of peak wind speed is randomly selected by the HOMER.

2.4. Diesel

The latest non subsidized diesel price is US$0.18/L in Iran (NIOPDC, 2016). It is eventually estimated US$0.21/L including transportation and storage costs. Since the diesel is a national product as a low price fuel, it can be considered as an advantage from economical point of view. But, as mentioned previous, the prevention of the air pollution is one of the most important motivation of MGs appearance. In this sense, the diesel usage should be restricted.

2.5. Economic inputs

The project lifetime is considered to be 25 years with an annual discount rate of 4%. The system fixed capital cost includes in stores managing, labor wages, different civil constructions, required licenses, administration and government approvals and other miscellaneous costs (Sen and Bhattacharyya, 2014). It is considered to be $30,000 for the whole project, and the fixed operation and maintenance cost of the system is estimated as $500/year.

3. System description and specification

The proposed MG is made up of eight main components including a diesel generator (DG), a fuel cell (FC), an electrolyzer, a

Table 5
Description and economic and technical specification for the components of the proposed MG.

Description	Specification	Description	Specification
PV modules		**Fuel cell**	
Model	PV-MF100EC4	Type	PEMFC
Rated power	250 kW	Rated power	200 kW
Capital cost	$7300/kWh	Capital cost	$3000/kW
Replacement cost	$2974/kWh	Replacement cost	$2500/kW
Operating and maintenance cost	$10/kWh	Operating and maintenance cost	$0.02/kWh
Life time	25 yrs.	Life time	50000 hrs.
Temperature coefficient	− 0.5%/°C	Efficiency	50%
Derating factor	80%	**Electrolyzer**	
Wind turbine		Rated power	200 kW
Type	BWC Excel-S	Capital cost	$1900/kW
Rated power	10 kW dc	Replacement cost	$1400/kW
Capital cost	$30730	Operating and maintenance cost	$20/y
Replacement cost	$22900	Life time	15 yrs.
Operating and maintenance cost	$458/y	Efficiency	90%
Life time	15 yrs.	**Hydrogen tank**	
Storage battery		Rated power	300 kg
Type	Surrette 6CS25P	Capital cost	$1200/kg
Capital cost	$1229/single cell	Replacement cost	$100/kg
Replacement cost	$1229/single cell	Operating and maintenance cost	$15/y
Operating and maintenance cost	$10/y	Life time	25 yrs.
Diesel generator		**Inverter**	
Type	Perkins	Type	Leonics GTP519S
Rated power	250 kVA	Rated power	900 kW
Capital cost	$182.5/kW	Capital cost	$300/kw
Replacement cost	$175/kW	Replacement cost	$300/kW
Operating and maintenance cost	$0.03/h	Operating and maintenance cost	$10/y
Life time	15000 hrs.	Life time	10 yrs.
Minimum load ratio	30%	Efficiency	90%

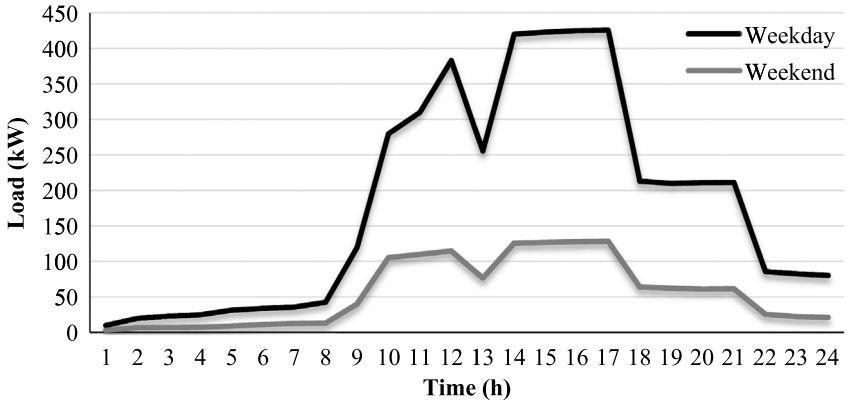

Fig. 1. A sample of the daily load profile for the studied CNC workshops set in weekday and weekend.

hydrogen tank, PV modules, WTs, batteries, and power converters as shown in Fig. 3(a). The MG can be operated in the grid-connected or islanded operation modes. Fig. 3(b) shows the configuration of the MG in the HOMER software. The descriptions of the selected components are presented in Table 5 and their characteristics are provided in the following subsections.

3.1. Sizing of the PV modules

In this study, the maximum installable PV capacity is considered 250kW which is approximately half of the peak load. In order to place PV panels in this project, the workshops roofs are used in addition to buy a certain place. The CNC workshops are stuck in each other and the MG designer should use the wasteland on the right side of the MG to place the majority of the MG equipment like the surplus PV panels than the roofs mounted. Recently, attention to the roof top PV panels, and researches on their applications are increased (Dabaieh et al., 2016; Plangklang et al., 2016; Feng et al., 2015). Every workshop has the area of 160 m^2. Therefore, the proposed MG has the area of 1500 m^2 considering the workshop sloping roofs and PV panels gap. Reduced cost due to using the workshops roof for PV panels' placement is considered in their replacement cost because the HOMER software does not prepare any option for this condition. The selected PV module is a 36-cell polycrystalline (PV-MF100EC4) which is rated at 100 W with the area of 0.81 m^2 (Ngan and Tan, 2012). Hence, the roof top PV capacity is calculated 185.2 kW, and the rest of the 64.8 kW PV capacity should be placed on the bought ground. The capital cost of the PV panels is considered $7300/kWh (Brochure, 2016), and the replacement cost is calculated $2974/kWh.

3.2. WT characteristics

In this simulation, the BWC Excel-S, 10 kW DC type WT model is chosen. The BWC Excel-S is a modern 10 kW WT designed for high reliability, low maintenance, and automatic operation in unfavorable weather conditions (Bergey, 2016). Table 6 shows the technical characteristics of this WT. The operating and maintenance cost is assumed to be 2% of the replacement cost in the economic assessment. Reader can see the power–speed characteristic and other information of the WT in the website (Bergey, 2016).

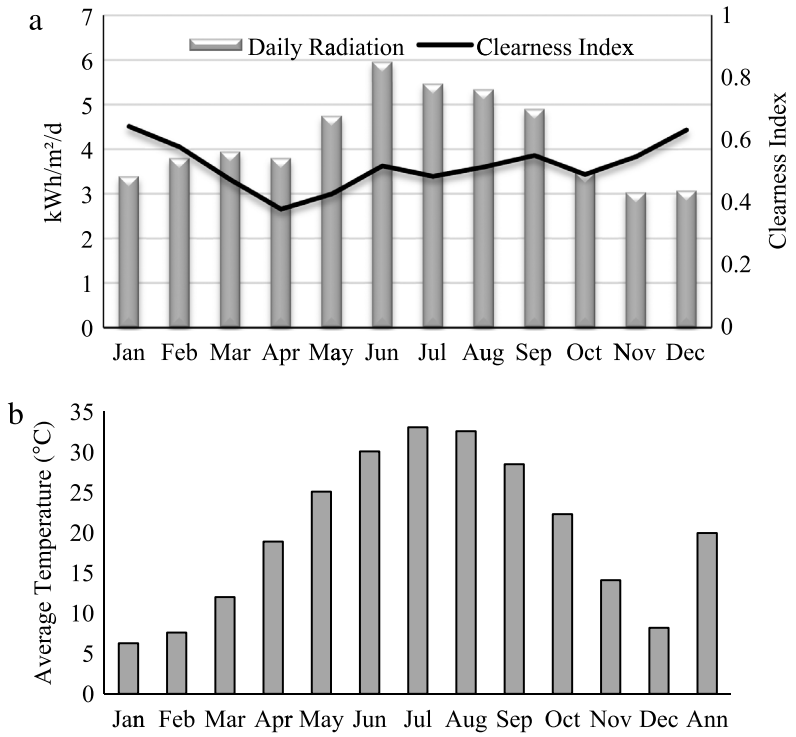

Fig. 2. The Monthly Averaged data for the location of Shad-Abad, Iran. (a) Solar radiation and clearness index. (b) Air temperature at 10 m above the surface of the earth.

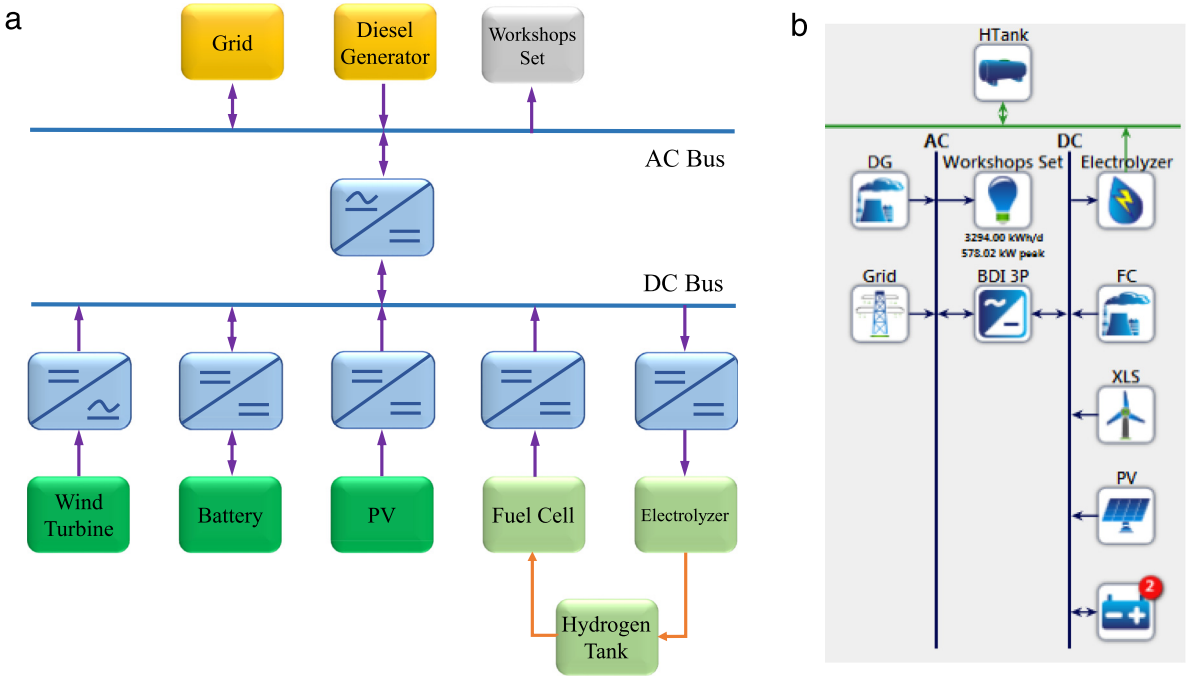

Fig. 3. (a) Block diagram of the proposed MG. (b) The configuration of the proposed MG in HOMER.

3.3. Storage battery

The Surrette 6CS25P battery model is chosen as the energy storage device in this simulation (Surrette, 2016). The characteristics of the battery are shown in Table 5. In order to produce higher energy capacity, 10 batteries are connected in series, which form a battery string. Each battery string can produce 70 kWh of electricity. Two separate energy storage entities are applied to increase the MG reliability and flexibility. In MGs with RESs, the roll of energy storage devices is undeniable especially in the cases of non-dispatchable generation compensation, and load-frequency control (Yang et al., 2016; Moradi et al., 2016; Coelho et al., 2016). In each energy storage entity, number of battery strings can be chosen from 0 to 12 to assess the MG performance in different cases.

3.4. Diesel generator

In this study, the 250 kva Perkins DG model with a capacity of 200 kw is selected to supply the half of the load such as the sensitive load in the emergency. the initial capital cost of the dg is $182.5/kw Perkins, 2016). Replacement and operational costs are assumed $175/kW and $0.030/h, respectively. Operating lifetime is also considered as 15,000 h.

3.5. Fuel cell

The low-temperature proton-exchange membrane FC (PEMFC), which is known for having great potential in hybrid energy system applications (Wang et al., 2005), is chosen in this study. The types of FC technology, DC–DC converter, compressor and ancillary equipment establish the finished FC cost (Ashourian et al., 2013). According to different prices of FCs due to their new technologies (Fuel cell stacks, 2016), FC prices are varied from $3000/kW to $6000/kW. In this study, the capital, replacement and operational costs are estimated to be $3000/kW, $2500/kW, and $0.02/kWh, respectively (Ashourian et al., 2013). Five different sizes of FCs, rating from 0 to 200 kW, are considered in the simulations. The lifetime and efficiency of the FC are considered to be 50,000 h and 50%, respectively.

3.6. Electrolyzer

Against to the electrochemical reaction that is occurred in a FC to provide the DC power, an electrolyzer converts electrical energy into chemical energy which is stored in hydrogen (Arkin and Duffy, 2001). The recent electrolyzer cost is $1500-$3000 per kW (Ashourian et al., 2013). Although, the cost will expected to decrease in next years by developing the electrolyzer manufacturing technology. In this study, based on the fuel cell sizes, various sizes of electrolyzer are considered from 0 to 200 kW with 90% efficiency. The capital and replacement prices are considered as $1900/kW and $1400/kW, respectively. The electrolyzer lifetime and maintenance/operation cost are estimated to be approximately 15 years and $20/year, respectively. The electrolyzer should be forced on 2 h per weekdays due to technical constraints.

3.7. Hydrogen Tank

The output electrolyzer hydrogen is stored in a hydrogen tank to supply the FC in other times. The cost of keeping 1 kg of hydrogen capacity in the hydrogen tank is estimated to be $1200. In addition, the replacement and maintenance costs are estimated to be $1100/kg and $15/year, respectively. Various sizes of the tank are up to 300 kg which are considered in four steps. The lifetime of the hydrogen tank is also estimated to be 25 years. The level of the tank at the start of simulation is considered 10% of the rated capacity.

3.8. Inverter

Since more of RESs generate the DC electric power and more of loads consume the AC electric power, the DC power should be converted to the AC power using inverters. The sizing of the inverter is based on the rated power of DC-side energy sources which is provided by the HOMER optimizing. In this study, the inverter model Leonics GTP519S with a capacity of 900 KW is selected that its DC bus voltage is 700 V. For all inverter sizes, the efficiency is presumed to be 90%. Both capital and replacement prices of the inverter are $300/kW, and its lifetime is up to 10 years. Various sizes of the inverter, rated up to 900 kW, are considered in 5 steps for the optimization.

3.9. Grid

Since the electricity market pricing is not applied in Iran, and prices are specified nationally, this energy is not expensive in comparison to countries with deregulated power systems. Therefore, the grid is the main power component in this MG. Three rates off-peak, normal, and peak are defined for the load. Since the under study MG is in an industrial region, peak hours are 9–12 and 14–17, normal hours are 12–14 and 17–19, and other hours are considered as off-peak. Purchase/sell tariffs from/to the grid for the MG are given in Table 7. These prices are taken from Great Tehran Electrical Distribution Company for industrial consumers and Renewable Energy Organization of Iran (Industrial power tariffs, 2016; Renewable energy tariffs, 2016). The sell price is constant in all situations and it is much larger from purchase prices to encourage private renewable electricity sellers. It is worth mentioning, the reliability of the grid is taken into account also. The average failure frequency for industrial regions is considered 10/year with the average repair time of 4 h.

4. Economic analysis

The HOMER approach in ranking of the optimization results is based on the total net present cost (NPC). The NPC is the present value of the MG installation and operation costs over its lifetime in the project that is calculated as follows:

$$NPC = \frac{C_{ann,tot}}{CRF\ (i, N)}, \tag{1}$$

where $C_{ann,tot}$ is the total annual cost of the MG in $/year and $CRF\ (i, N)$ is the capital recovery factor that is a ratio used to calculate the present value of a series of equal annual cash flows and is given by:

$$CRF\ (i, N) = \frac{i(1+i)^N}{(1+i)^N - 1}, \tag{2}$$

where i is the real interest rate and N is the project life time in year. The real interest rate itself is obtained from the nominal interest rate (i') and annual inflation rate (f) as follows:

$$i = \frac{i' - f}{1+f}. \tag{3}$$

This equation indicates the effectiveness of projects performing in the condition with the large annual inflation rate and small nominal interest rate. The nominal interest rate and annual inflation rate in Iran are respectively reported 21% for industrial projects, and 15% in February 2015 (Nominal interest rate, 2016). Thus, the real interest rate is calculated 5.2% using Eq. (3). The project lifetime is considered as 25 year.

The HOMER uses levelized cost of energy (COE) as an output variable index. The COE is the average cost per kWh of useful electrical energy produced by the MG. The COE is calculated in MGs without any thermal load in the following manner:

$$COE = \frac{C_{ann,tot}}{E_{srv}}, \tag{4}$$

where E_{srv} is the total electrical load served in the MG in kWh/year. Although, the COE is a convenient index which can compare different configurations, the HOMER does not rank them based on the COE.

5. Numerical results and discussion

The simulations are executed for the proposed MG, shown in Fig. 3, and the HOMER search space is given in Table 8. The simulation is done with a project lifetime of 25 years. The MG planning is done focusing on three main objectives:

- Minimum cost of the MG construction and operation
- Using available capacity to apply maximum renewable energies such as wind and solar, and subsequently to access minimum air pollution
- Assurance of sustainable and secure operation of CNC machines as sensitive loads using energy storage supplies and DGs as dispatchable supplies.

Due to the cheap grid electricity in Iran and its relative reliability, a big percent of the electricity is considered to produce by the grid. This is desirable in the viewpoint of the first objective. For the second objective, the maximum penetration of RESs is desired. And, for the third objective, existence of a battery entity, a DG or both of them is necessary. According to this planning strategy, simulation results are obtained and the discussions about them are given in the following five subsections.

5.1. Top nine plans with different constructions

Nine reasonable and preferable plans which provide desirable optimization results are shown in Table 9. The HOMER simulation results include a number of feasible but not reasonable results such as existence of the hydrogen tank without the electrolyzer and FC or existence of the hydrogen tank and electrolyzer without the FC. These results have been eliminated to access reasonable plans. The plans are sorted from 1 to 9 based on the microgrid NPC in Table 9. One of the first deductions is the less NPC for plans without battery than equivalent plans with battery. In addition, the FC and its requirements consist of the hydrogen tank and electrolyzer cause extremely-uneconomical plans, thus plans 7, 8 and 9 are eliminated at first. In order to select the best plan, the second and third objectives of the MG planning have also to be taken account. Fig. 4 shows per unit values of the NPC, COE, DG pollution, and renewable fraction that are calculated by dividing real values by the maximum value of each index respectively. These diagrams show the variation of different indices with respect to each other for the selected plans. The NPC and COE indices have approximately the same increase because of their similar behavior in the economic assessment. The index of the DG pollution, equivalent to the DG production, shows plans 3 and 4 have the maximum DG production and plans 5 and 6 have not any DG capacity. Another interesting result, which this index shows, is the less DG pollution of plan 2 than plan 1. The renewable fraction index has uniform rate except in plans 5 and 6. In these two plans, RESs compensate DG absence. Consequently, plans 1 and 2 have the minimum NPC with the difference of $0.2M and plans 5 and 6 have the maximum renewable fraction, zero air pollution, and greater NPC. Plans 1 and 5 have no battery that is good reason for their deletion. Finally, it can be said that plan 2 is the best plan with almost the minimum NPC in the presence of battery and DG for ensuring of sensitive loads electrification.

In this study, two battery sets with half of the required battery capacity are considered as shown in Fig. 3(b) to increase reliability. If one of them has an outage, because of an inner fault or maintenance, another one supports storage requirements of the MG. Nevertheless, in the HOMER, two distinct battery entities have not any effect in optimization results than one entity. Thus, one battery entity with the maximum required storage capacity is considered in the next simulations.

In the next scenarios, plan 2 is selected as a base plan to study the minimum renewable penetration, PV development versus WT development, impact of battery unit increase on the MG planning, and reliability assessment. All the next four scenarios are selected to check three MG planning objectives mentioned above.

Table 6
Technical characteristics of BWC Excel-S WT (Bergey, 2016).

Rated power	8.9 kW at 11 m/s
Annual average energy	13800 kWh at 5 m/s
Rated wind speed	11 m/s
Cut-in wind speed	2.5 m/s
Furling wind speed	14–20 m/s
Maximum design wind speed	60 m/s
Number of rotor blades	3
Rotor diameter	7 m
Hub height	24–49 m (25 m in simulations)
Rated sound level	42.9 dB

Table 7
Grid purchase and sell tariffs.

	Buying energy cost ($/kWh)	Selling energy cost ($/kWh)
Peak	0.0155	0.16
Normal	0.0047	0.16
Off-peak	0.0011	0.16

5.2. Minimum renewable penetration with and without battery

In this scenario, the minimum renewable fraction is changed from 10 to 40 by step size of 5. As mentioned before, the impact of minimum renewable fraction is obtained on the indices of plan 2. Fig. 5 shows these indices including the NPC, COE, DG fuel, grid purchase, and grid sold. According to NPC and COE, the cost of MG planning increases approximately linearly with the increase in the renewable fraction that is equivalent to the decrease in grid purchase. This decrease is visible in the grid purchase curve. Generally, RESs are much cleaner than the grid energy but they are more expensive. Nevertheless, the local increase in the grid purchase for the renewable fraction of 15% to 20% is due to the large decrease in the DG production. The renewable fraction of less than 20% is not suitable in the viewpoint of the second and third MG planning goals, because the RESs penetration is low and the DG pollution is high. In this situations, the DG tries to produce large amounts of electricity to sell the grid. It can be deduced by observing DG fuel and grid sold curves which are almost on each other in the renewable fraction of less than 20%.

On the other hand, other indices can be checked that have better behavior in the less renewable fractions. The excess energy and unmet load are two indices that have lower amounts in the renewable fraction of less than 20%. These results are shown in Fig. 6. The less excess energy and unmet load for less renewable fractions is due to the large DG production. These indices cannot proof the efficiency of the less renewable fractions because the excess energy and unmet load amounts are not enormous generally and their increase with the renewable fraction increase is low and non-uniform. Existence of the two maximum points in the unmet load curve is due to the DG production decrease in the first step and complete DG outage in the second step. Besides, the excess energy becomes less using the battery (plan 2 instead of plan 1). According to Fig. 6, the excess energy of 35% renewable fraction with the battery equals the same amount of 17% renewable fraction without the battery. On the other hand, the battery has no effect on the unmet load for the renewable fraction of bigger than 20% because of the battery discharge limitation. Therefore, the best RESs penetration rate is economically and technically the value between 20% and 30%.

5.3. PV development versus WT development

By choosing the second plan of the main simulation in Section 5.1, the PV and WT developments and their effects on the NPC are outlined. Fig. 7 shows the normalized NPC for the increase of the WT and PV nominal capacities in steps of 30 kW. It is obvious,

Table 8
Values of all optimization variables.

Converter (kW)	Grid Purchase (kW)	H Tank (kg)	Electrolyzer (kW)	Battery 1 (n)	Battery 2 (n)	FC (kW)	DG (kW)	PV (kW)	WG (n)
0	0	0	0	0	0	0	0	0	0
300	1000	100	100	40	40	100	50	60	7
600		200	200	80	80	200	100	120	14
900				120	120		150	180	21
							200	250	

Table 9
The best optimization results of the MG planning.

Plan	PV (kW)	WT (n)	FC (kW)	DG (kW)	Battery (n)	Grid (kW)	Electrolyzer (kW)	H Tank (kg)	Converter (kW)	NPC ($)
1	60	21	–	50	–	1000	–	-	300	1 679 098
2	60	21	–	50	80	1000	–	-	300	1 871 337
3	250	–	-	100	–	1000	–	-	300	2 126 354
4	250	–	-	100	80	1000	–	-	300	2 353 911
5	250	7	–	-	–	1000	–	-	300	2 568 618
6	180	21	–	-	80	1000	–	-	300	2 779 870
7	120	21	100	50	–	1000	200	100	300	3 272 760
8	120	21	100	50	80	1000	200	–	300	3 316 866
9	120	21	200	50	80	1000	200	100	300	3 672 796

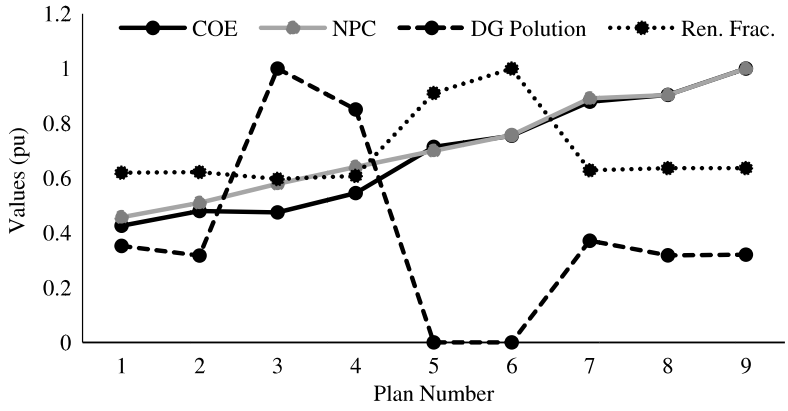

Fig. 4. Per unit values of NPC, COE, DG pollution and renewable fraction for the selected nine plans.

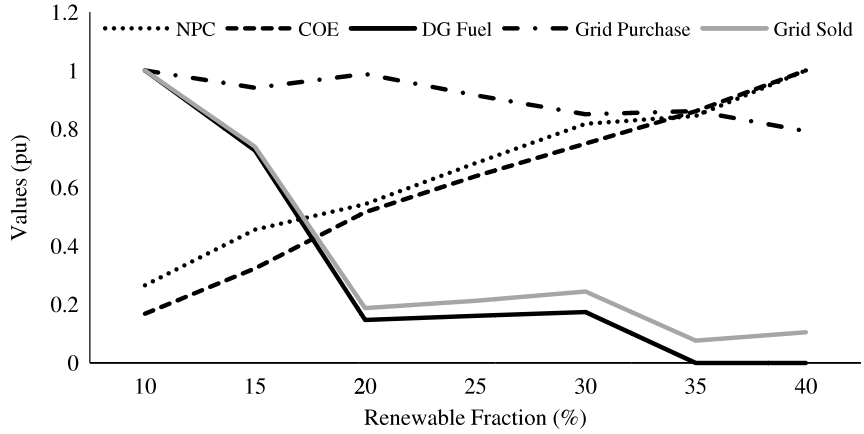

Fig. 5. Per unit values of NPC, COE, DG fuel, grid purchase and grid sold for different renewable fractions.

the NPC increase slope for the PV capacity is more than it for the WT capacity. Thus, in the MG development plan, the WT has a priority in terms of costs. However, we should take account other aspects such as the visual and auditory pollution in the development plan. Environmental concerns are very important aspects of an RES and its development that have been recently studied more and more (Premalatha et al., 2014; Onakpoya et al., 2015). The HOMER software can consider some environmental concerns such as the emission amounts of the air pollutants due to the grid and DG but it does not consider other environmental concerns such as visual, auditory, and marine pollutions. The MG planner should add this constraints out of the HOMER environment.

5.4. Impact of number of batteries on the MG planning

In this scenario, the number of battery units are increased from 40 to 160 to investigate its impact on the NPC and excess electricity.

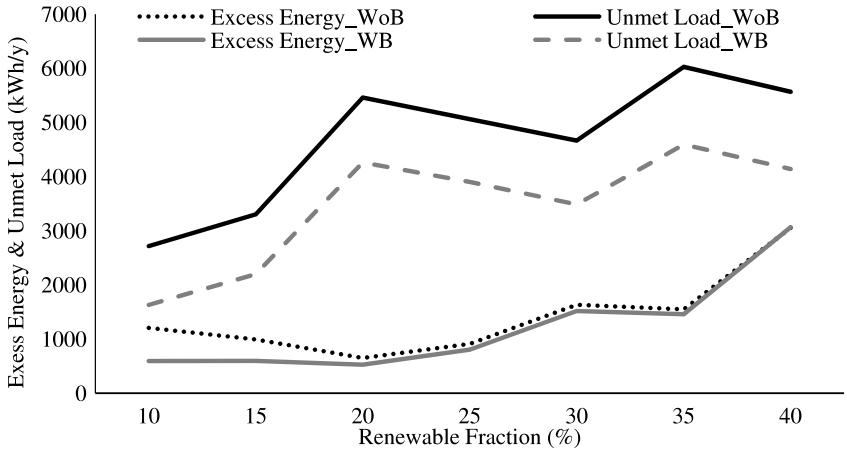

Fig. 6. Excess energy and unmet load with and without battery (plans 2 and 1, respectively) for different renewable fractions.

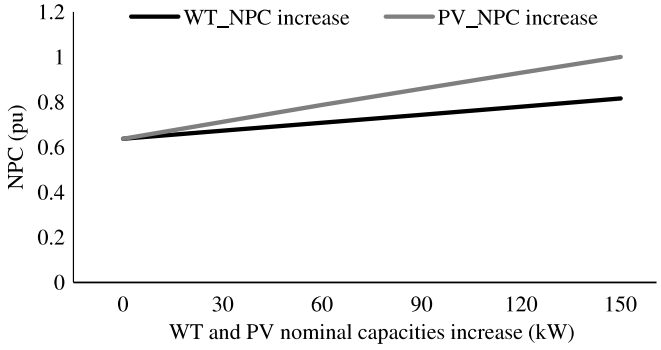

Fig. 7. Normalized NPC for WT and PV nominal capacities increase to 150 kW.

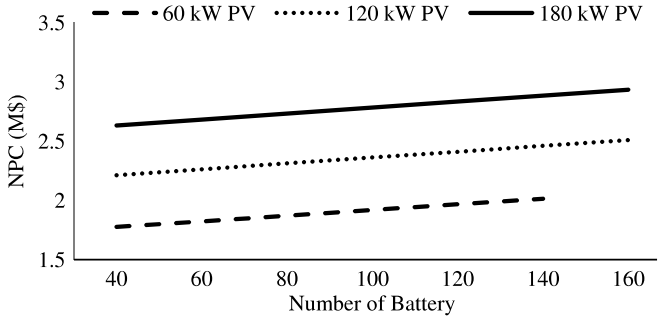

Fig. 8. NPC for three different PV capacities 60, 120 and 180 kW, and different number of batteries.

Fig. 8 shows the NPC for three different PV capacities 60 kW, 120 kW, and 180 kW. In all situations, the NPC increases linearly with increasing the batteries number. The plan with 60 kW PV capacity is not feasible for larger than 140 batteries. In the economical point of view, the best selection is the less feasible PV and battery capacities. Fig. 9 shows the excess electricity and its changes with the number of batteries. The plans with 180 kW PV capacity have the larger excess electricity whereas the plans with 60 kW and 120 kW PV capacities have the less excess electricity. Excess electricity rate is low for increasing of batteries from 40 to 100 and it has the increasing rate from 100 to 160 batteries. Therefore, the choice of 40 to 100 batteries and a PV capacity less than 120 kW is more efficient.

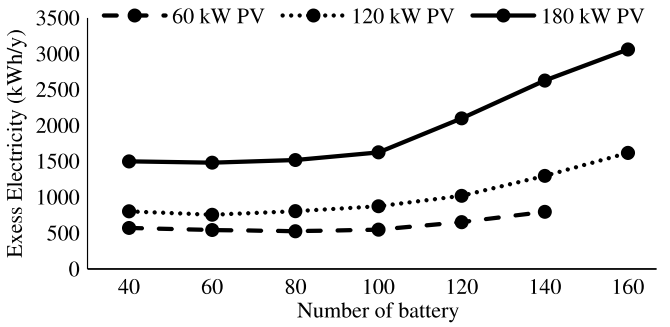

Fig. 9. Excess electricity for three different PV capacities 60, 120 and 180 kW, and different number of batteries.

5.5. Reliability assessment

Since the MG has sensitive loads such as CNC machines, the reliability and its assessment is necessary. The Energy not supplied (ENS) as a common reliability index, which is called unmet load in HOMER, is used in this study. The normalized values of the excess electricity, unmet load and capacity shortage are presented in Fig. 10 for different repair times. The unmet load, same ENS, increases generally with the repair time increase. According to the grid purchase and sold curves, two maximum points and one minimum point are expected in the minimum repair times of 5, 8 and, 7 h of the unmet load curve respectively. The capacity shortage curve is fitted on the unmet load curve because they have same behavior and the curves are normalized. The unmet load is of energy in kWh/y and the capacity shortage is of power in kW. According to Fig. 10, a general increase is seen in the excess electricity. Besides, the severe grid purchase decrease and grid sold increase for the repair times of 4 to 6 h result in the minimum excess electricity in the repair time of 6 h. Although some of these minimum or maximum points have not any scientific reason, they exist due to the randomness of the reliability assessment. Finally, the best repair time is the possible minimum repair time economically and technically.

6. Conclusion

Many simulations were executed in the HOMER software to plan a developing MG including a set of CNC workshops as load, renewable and non-renewable energy sources and energy storage supplies in Shad-Abad industrial estate, Tehran, Iran. Three main

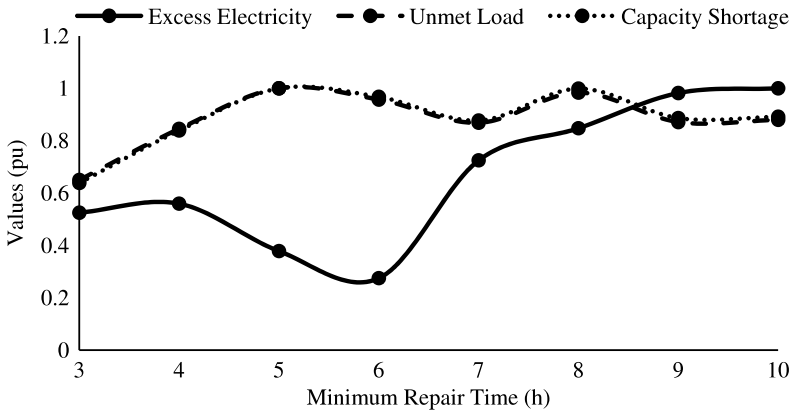

Fig. 10. Normalized values of excess electricity, unmet load and capacity shortage for different repair times.

objectives are considered in the MG planning including minimum construction and operation MG costs, using available capacity to penetrate the possible highest renewable energy and subsequently produce minimum air pollution, and assurance of sustainable and secure operation of the CNC machines as the sensitive loads. In order to realize these objectives, the MG was simulated in five scenarios. In the first scenario, the best plan has the minimum NPC about $1.87M in the presence of 80 battery units and 50 kW DG for assurance of the sensitive loads electrification. By simulating the second scenario, it was deduced that the best RESs penetration is economically and technically in the range of 20% to 30%. In the third scenario, the results showed that the WT development has a priority in terms of costs against to the PV development, but we should also pay attention to the environmental constraints. The sensitive analysis, presented in the fourth scenario, results in the choice of 40 to 100 battery units and the PV capacity less than 120 kW. Moreover, increase in the PV capacity from 60 to 180 kW results in approximately 90000 kg/y decrease in the CO_2 emission. The last scenario came our attention on the reliability. Many indices such as the unmet load/ENS, capacity shortage, excess electricity, grid purchase, and grid sold are affected badly of the repair time increase. The impact of the inner producers on the MG reliability improvement is also undeniable.

In addition to the MG planning which is presented in this paper, the control and operation of this MG can be considered in the future works.

References

Arkin, A., Duffy, J., 2001. Modeling of PV, electrolyzer and gas storage in a stand-alone solar-fuel cell system. In: Forum-Proceedings. American solar energy society & the American institute of architects, pp. 253–258.

Ashourian, M.H., et al., 2013. Optimal green energy management for island resorts in Malaysia. Renew. Energy 51, 36–45.

Babazadeh, M., Karimi, H.R., 2013. A robust two-degree-of-freedom control strategy for an islanded microgrid. IEEE Trans. Power Deliv. 28 (3), 1339–1347.

Bahramara, S., Parsa-Moghaddam, M., Haghifam, M.R., 2016. Optimal planning of hybrid renewable energy systems using HOMER: A review. Renew. Sustain. Energy Rev. 62, 609–620.

Bergey, 2016. Excel-S 10 kW turbine specifications. http://bergey.com/.

Bevrani, H., Francois, B., Ise, T., 2017. Microgrid Control: Dynamics and Control. WILEY.

Botelho, A., Pinto, L.M.C., et al., 2016. Social sustainability of renewable energy sources in electricity production: an application of the contingent valuation method. Sustainable Cities and Society.

Brochure, 2016. PV-MF100EC4 specifications. http://pv.energytrend.com/pricequotes.html..

Coelho, V.N., et al., 2016. Multi-objective energy storage power dispatching using plug-in vehicles in a smart-microgrid. Renew. Energy 89, 730–742.

Dabaieh, M., Makhlouf, N.N., Hosny, O.M., 2016. Roof top PV retrofitting: A rehabilitation assessment towards nearly zero energy buildings in remote off-grid vernacular settlements in Egypt. Sol. Energy 123, 160–173.

Demiroren, A., Yilmaz, U., 2010. Analysis of change in electric energy cost with using renewable energy sources in Gokceada, Turkey: an island example. Renew. Sustain. Energy Rev. 14 (1), 323–333.

Feng, C., et al., 2015. A novel solar multifunctional PV/T/D system for green building roofs. Energy Convers. Manage. 93, 63–71.

Fuel cell stacks, 2016. http://fuelcellstore.com/.

HOMER help, 2016. http://www.homerenergy.com/.

Industrial power tariffs, 2016. http://www.tbtb.co.ir/en/home.

Kobayakawa, T., Kandpal, T.C., 2016. Optimal resource integration in a decentralized renewable energy system: Assessment of the existing system and simulation for its expansion. Energy Sustain. Dev. 34, 20–29.

Lau, KY., Yousof, M.F.M., et al., 2010. Performance analysis of hybrid photovoltaic/diesel energy system under malaysian conditions. Energy 35, 3245–3255.

Leung, D., Caramanna, G., Maroto-Valer, M.M., 2014. An overview of current status of carbon dioxide capture and storage technologies. Renew. Sustain. Energy Rev. 39, 426–443.

Li, M., et al., 2016. A feasibility study of microgrids for reducing energy use and GHG emissions in an industrial application. Appl. Energy 176, 138–148.

Louie, H., 2016. Operational analysis of hybrid solar/wind microgrids using measured data. Energy Sustain. Dev. 31, 108–117.

Manas, M., 2015. Renewable energy management through microgrid central controller design: An approach to integrate solar, wind and biomass with battery. Energy Rep. 1, 156–163.

Moradi, M.H., Eskandari, M., Hosseinian, S.M., 2016. Cooperative control strategy of energy storage systems and micro sources for stabilizing microgrids in different operation modes. Int. J. Electr. Power Energy Syst. 78, 390–400.

Morinec, A.G., 2000. Power quality considerations for CNC machines: grounding. In: Industrial and Commercial Power Systems Technical Conference, Papers Presented at the 2000 Annual Meeting. IEEE.

Morinec, A.G., 2002. Corrections to power quality considerations for CNC machines: grounding. IEEE Trans. Ind. Appl. 38 (2), 615.

Ngan, M.S., Tan, C.W., 2012. Assessment of economic viability for PV/wind/diesel hybrid energy system in southern Peninsular Malaysia. Renew. Sustain. Energy Rev. 16 (1), 634–647.

NOAA, 2016. National oceanic and atmospheric administration. http://www.esrl.noaa.gov/gmd/ccgg/trends.

Nominal interest rate, 2016. http://www.cbi.ir/default_en.aspx#2.

Olatomiwa, L., 2016. Optimal configuration assessments of hybrid renewable power supply for rural healthcare facilities. Energy Rep. 2, 141–146.

Onakpoya, I.J., et al., 2015. The effect of wind turbine noise on sleep and quality of life: a systematic review and meta-analysis of observational studies. Environ. Int. 82, 1–9.

Peerapong, P., Limmeechokchai, B., 2017. Optimal electricity development by increasing solar resources in diesel-based micro grid of island society in Thailand. Energy Rep. 3, 1–13.

Perkins, 2016. 250 kVA diesel generator, 50 Hz. http://www.americasgenerators.com/.

Plangklang, B., Thanomsat, N., Phuksamak, T., 2016. A verification analysis of power quality and energy yield of a large scale PV rooftop. Energy Rep. 2, 1–7.

Premalatha, M., Abbasi, T., Abbasi, SA., 2014. Wind energy: Increasing deployment, rising environmental concerns. Renew. Sustain. Energy Rev. 31, 270–288.

Prodromidis, G.N., Coutelieris, F.A., 2010. Simulation and optimization of a stand-alone power plant based on renewable energy sources. Int. J. Hydrog. Energy 35 (19), 10599–10603.

Renewable energy tariffs, 2016. http://www.suna.org.ir/en/home.

Sen, R., Bhattacharyya, S.C., 2014. Off-grid electricity generation with renewable energy technologies in India: An application of HOMER. Renew. Energy 62, 388–398.
Sorensen, B., 2011. Renewable Energy: Physics, Engineering, Environmental Impacts, Economics & Planning. Elsevier.
Surface meteorology, 2016. Solar energy and wind speed. https://eosweb.larc.nasa.gov/sse/.
Surrette, 2016. 6-CS-25PS solar battery. http://webosolar.com/store/en/75-deep-cycle-batteries.
The National Iranian Oil Products Distribution Company, 2016. https://www.niopdc.ir/en/home.
Twidell, J., Weir, T., 2015. Renewable Energy Resources. Routledge.
Vasconcellos, A.B., et al., 2010. Efficiency and power quality in a drive system driving machine. In: 14th International Conference on Harmonics and Quality of Power (ICHQP). IEEE.
Wang, C., Nehrir, M.H., Shaw, S.R., 2005. Dynamic models and model validation for PEM fuel cells using electrical circuits. IEEE Trans. Energy Convers. 20 (2), 442–451.
Yang, L., et al., 2016. Energy regulating and fluctuation stabilizing by air source heat pump and battery energy storage system in microgrid. Renew. Energy 95, 202–212.